81CH1675-8

1981

IEEE International Symposium

on

Electromagnetic Compatibility

August 18-20, 1981

University of Colorado

Boulder, Colorado

Rising to Greater Heights

PERSONNEL ELECTROSTATIC DISCHARGE: IMPULSE WAVEFORMS RESULTING FROM ESD OF HUMANS DIRECTLY AND THROUGH SMALL HAND-HELD METALLIC OBJECTS INTERVENING IN THE DISCHARGE PATH

W. Michael King
Electromagnetic Compatibility Advisor
Santa Monica, California 90402
(213) 395-5003

David Reynolds
Electromagnetic Compatibility Engineer
Digital Equipment Corporation
301 Rockrimmon Blvd. South
Colorado Springs, Colorado 80919

Abstract

In 1979, a paper (by King) was presented to the EOS/ESD Symposium (1) that broadly described various impulse waveform characteristics that were produced as a result of charging humans to a known voltage level, and measuring the Electrostatic Discharge (ESD) impulses by contacting the subjects to a known load in a specific evaluation condition. The paper explored ESD events only at initial charge levels of 5,000 Volts and 10,000 Volts, although a specific 7.5kV example was noted from a push-cart. In general, various waveforms were shown as measured that exhibited risetimes ranging between one nanosecond and a few tens of nanoseconds, with certain events stated to exhibit risetimes in the area of 300 picoseconds, although the photographic data provided displayed an obvious 'ring' in the measurement equipment or test setup. This 'ring' made full characterization of the super-fast events difficult. In addition, the 1979 paper noted that multiple ESD impulses were encountered during the study effort, with the multiple impulses derived from what had been initially perceived as a single event from a single initialization (charge) level.

This paper was developed during ESD waveform research conducted during 1980-81, representing an extension of the previous effort, and based on a similar test methodology with improved stability at higher frequencies. The focus of this effort was to determine the various ESD waveform characteristics as produced across a full spectrum of initializing charge levels. Emphasis is placed on displaying the ESD waveforms and waveform modifications that are encountered as the amplitude level of the initializing charge is incrementally increased, and on displaying the various components that are inherent within each 'event' which exist within a framework of multiple impulses. Using fundamentally a wide bandwidth measuring system, the waveforms and waveform components exhibiting risetimes faster than one nanosecond are explored and expanded for clear presentation. Variations in the waveforms are provided to describe both the human (finger-tip) direct event characteristics as well as the event spectrum when a small hand-held metallic object is intervening in the discharge path. (A small metallic object consists of a key, coin, writing pen, ring or screwdriver).

The conceptual goal of this effort was to provide sufficient information derived from actual ESD events to be eventually utilized as a base of characterization for the development of ESD simulation equipment, under the premise that electronic systems would exhibit equal response to test simulators providing similar waveforms to those found in this study as measured in an identical test (measurement) system. Empirical results that have been gathered during evaluations of actual systems for susceptibility response have confirmed the premise that test simulators providing waveforms that match the results of this study will cause essentially identical susceptibility responses in the systems as the actual personnel ESD events that were applied to the system in the same manner. The correlation has been excellent. It is projected that a similar waveform match may be found useful to those concerned with component damage effects caused by ESD events during component handling.

Measurement Approach

The general approach of this study was aimed at determining the ESD impulse waveforms and waveform characteristics for the 'source' ESD events, rather than attempting to determine what resultant waveshapes may occur as propagated to a system. The basis of this approach was that if the 'source' ESD waveforms were known, and eventually simulated, then the ultimate systems under test would respond to the 'matched' (or simulated) 'source' waveforms in a manner essentially equal to the actual ESD events themselves. As indicated above, empirical data gathered on systems during comparative tests between actual-versus-simulated ESD events have confirmed this premise during confirmation tests of a simulator providing the 'matched' waveforms.

Based on experience provided during the 1979 effort, it was recognized that in order to measure the 'source' ESD waveforms it was necessary to 'capture' the transfer impedances between the human and the measurement system within the framework of a relatively low impedance reference plane system. Additionally, it was realized that the reference plane system would have to capture the distributive impedance represented through the 'feet-through-floor' plane as well as the surface plane which is expressed as a surface-to-surface distribution. The following describes the reference plane.

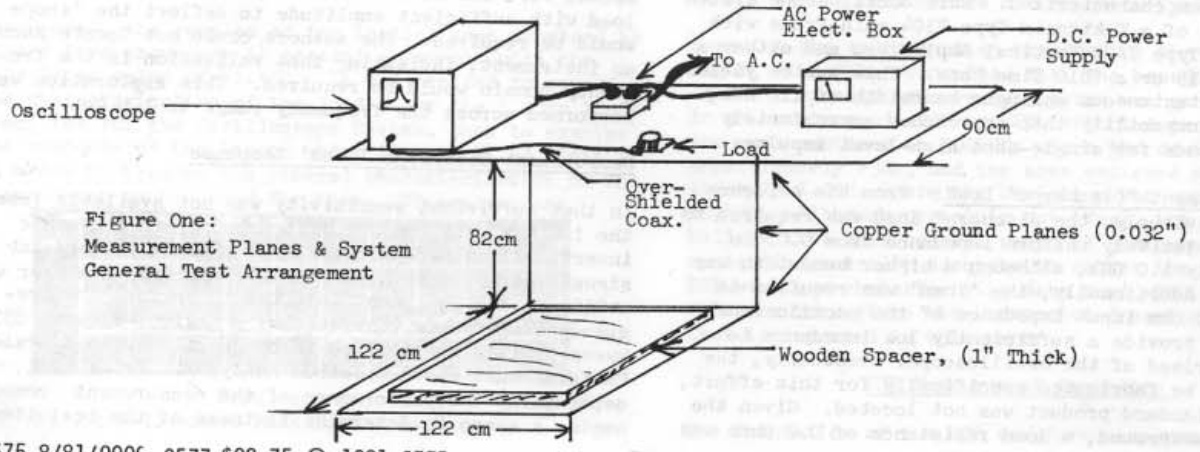

Figure One:
Measurement Planes & System
General Test Arrangement

CH1675-8/81/0000-0577 $00.75 © 1981 IEEE

Measurement Planes and System

The general arrangement of the measurement planes and the measurement system is illustrated by Figure One. The reference plane system was comprised of two horizontal planes fabricated from 0.032" copper which were interconnected vertically by a third plane which was seam-connected to the two horizontal planes. The first of the two horizontal planes was located on top of a bench surface, approximately 82cm above the floor surface. The measurements of this plane were approximately 244cm in length by 90cm in width. (The length was found helpful to minimize radiated susceptibility which had been encountered with the oscilloscope by permitting a position of the 'scope that was somewhat removed from the point of the ESD impulse application). The second horizontal plane measured approximately 122cm x 122cm and was placed directly on the floor surface. A spacer fabricated from wood was placed above the floor-plane to separate the surface of the shoes worn by the human under evaluation from the metal-surface of the floor plane. As a precaution, the humans were equipped with rubber-soled shoes available from a standard source. The thickness of the wood spacer was one inch.

The measurement system was placed on the bench-top plane. The measurement system consisted of a wide bandwidth oscilloscope, a wideband discharge 'load', a calibrated ±10% D.C. source that was utilized to charge the human subjects, an oscilloscope camera, and an electrical power distribution box. The power distribution box was mounted to the surface of the plane to facilitate connecting the plane to the ground of the building power system, and to provide a single ground distribution point for the oscilloscope A.C. power cord and the D.C. power supply. Between the discharge 'load' and the oscilloscope, a one meter length of coaxial cable (RG 223/u) was used for interconnection. This cable was overshielded with a tinned-copper braid shield to minimize radiated susceptibility responses from the oscilloscope. The tinned-copper braid also served to ground the front-end of the oscilloscope frame/casework to the plane, in that the overbraid was connected to plane at approximately 15cm intervals. The ground surface of the ESD 'load' was bolted directly to the plane. It should be noted that the output impedance of the D.C. power supply was established at 200 Megohms in order to prevent shock hazard to the personnel. The D.C. supply was metered to determine the D.C. level that was being applied to the personnel.

Measurement Oscilloscope: Based on the experience gained during the previous (1979) effort, it was known that an extremely wide bandwidth oscilloscope was required for these measurements with a write-enhanced CRT. At this writing, there is only one oscilloscope system that is known to the authors to be capable of measuring the full spectrum of ESD event waveforms that have been characterized. This oscilloscope system is comprised of a Tektronix Type 7104 main frame with a Tektronix Type 7A29 Vertical Amplifier, and either a Tektronix 7B15 or a 7B10 Time Base. This system yields a 'flat' instantaneous analogue bandwidth of 1.0 GHz, and a write capability that approaches approximately 200 picoseconds for single-shot high-level impulses.

Measurement 'Discharge' Load: From the evidence gathered previously, the discharge load was required to provide a relatively uniform impedance from D.C. to approximately 1.0 GHz, although a higher bandwidth was desirable. Additionally, the 'load' was required to match the 50 Ohm input impedance of the oscilloscope system, and provide a sufficiently low impedance to prevent overload of the oscilloscope. Eventually, the load had to be fabricated specifically for this effort, in that a standard product was not located. Given the empirical background, a load resistance of 0.2 Ohms was determined to be acceptable. This 0.2 Ohm load would provide a response of 1.0 Amperes per 100 millivolts when the 6db loss across the 50 Ohm matching resistor to the oscilloscope system was taken into consideration. The mechanical configuration of the load is shown below as Figure Two.

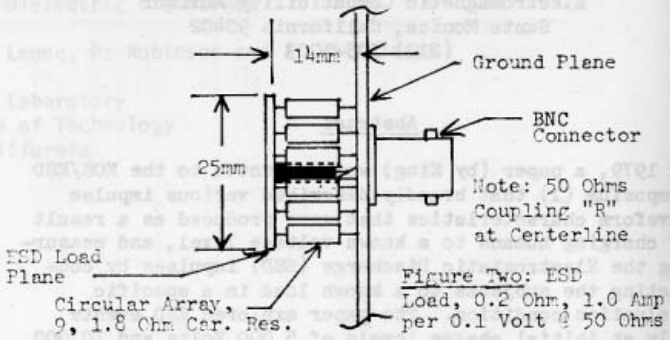

Figure Two: ESD Load, 0.2 Ohm, 1.0 Amp per 0.1 Volt @ 50 Ohms

As illustrated, the load consisted of a circular array of ½ watt carbon composition resistors by the Allan-Bradley Company. The circular array was comprised of nine resistors, measured at 1.8 Ohms each for a total of 0.2 Ohms. The resistors were soldered to a circular plate of copper which had an outside diameter of 25mm. The plate was drilled-through to pass-through and solder the resistor leads, which were arranged concentrically about the circumference with the diameter across the lead centers of 20mm. At the center of the plate, a 50 Ohm carbon composition resistor of the same manufacturer (actually a 47 Ohms rated resistor that was selected for its 50 Ohms actual value) connected the plate to a BNC connector that was mounted on the parallel ground plate. The separation between the circular plate and the ground plate was approximately 14mm. The ground plate was similarly drilled with a 20mm circular pattern in order to pass-through and solder the resistors. Immediately behind and centered with the 50 Ohm coupling resistor was a BNC connector, which was also soldered to the ground plate. The 25mm diameter circular plate served as the Electrostatic Discharge 'Load' surface for all measurements, although it was occasionally necessary to install a 20 db attenuator in series with the coaxial connection to the oscilloscope to facilitate higher amplitude measurements.

Measurement System Response

Initially, it was intended to validate the load and measurement system response in the time domain by applying a rapid step-function impulse to the surface of the load in order to investigate for 'ringing' or other impedance disruptions. Unfortunately, the bandwidth need indicated that if validation of a 200 to 500 picosecond risetime response was to be accomplished, an impulse generator providing approximately a 50 picosecond risetime with the ability to drive a 0.2 Ohm load with sufficient amplitude to deflect the 'scope would be required. The authors could not locate such an instrument, indicating that validation in the frequency domain would be required. This exploration was performed across the frequency range to 1.5 GHz.

Measurement Discharge 'Load' Response

In that sufficient sensitivity was not available from the 1.0 GHz Oscilloscope System to permit a dynamic insertion loss sweep of the load with a standard lab signal source, a highly-sensitive spectrum analyzer was utilized. The equipment selected to perform the frequency range scans consisted of a Hewlett-Packard 8350A Sweep Oscillator utilized in conjunction with a Hewlett Packard Model 8568A Spectrum Analyzer. Prior to determining the performance of the measurement components, a sweep to determine flatness of the test items

response was performed. To perform this evaluation, the Sweep Oscillator was connected to the Spectrum Analyzer, with the following response observed from 0-1.5 GHz.

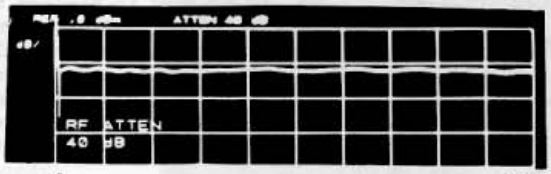

0 1.5GHz

Note: Scale 10db/Div.

Fig. 3 - Response of Oscillator to Analyzer

The profile demonstrated by Figure Three above indicates that the combination of the Sweep Oscillator and the Spectrum Analyzer were mutually within the specified criteria for flatness of ±1db each, ±2db total.

Next, the measuring equipment noted above was setup to perform an insertion loss scan on the ESD 'Load'. In order to partially isolate the Sweep Oscillator from the very low impedance of the load (0.2 Ohms), a 6db attenuator was installed between the Oscillator and the discharge plate of the load. The load was setup in a coaxial test fixture to minimize coupling losses between the oscillator and the load surface, with a type 'N' connector facilitating the interconnection. The total test arrangement is described by the following diagram.

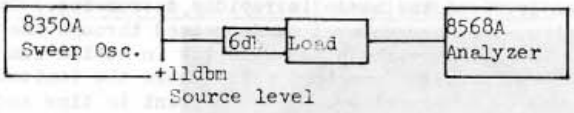

Fig. 4 - Insertion Loss Test of Load

A calculation was performed to determine the probable insertion loss that would result in this arrangement. The total insertion loss, including the 6db pad as terminated to the 0.2 Ohm load was calculated as 51.4db. The Sweep Oscillator was adjusted to an output level of +11dbm, with the Analyzer reference line setup at -10.0 dbm. The following insertion loss scan resulted across the frequency range of 0 - 1.0 GHz.

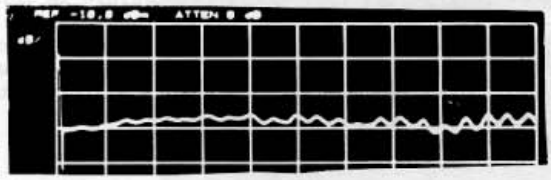

0 Frequency 1.0GHz

Fig. 5 - Initial Loss Scan of 0.2 Ohm Load
Displayed: -40 to -36dbm from +11dbm Ref.
Insertion Loss Result: -51dbm to -47dbm

In general, the results of the initial scan provided by Figure Five above are in general agreement with the calculated value of 51.4db. It was decided to expand the characterization of the load above the 1.0GHz limit specified for the Oscilloscope System, then to examine the response of the 'scope above its specified limit in order to broaden the general characterization of the measurement system used for these ESD evaluations.

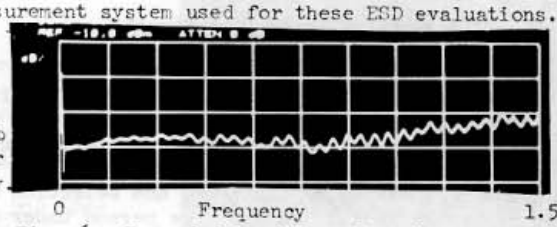

0 Frequency 1.5GHz

Fig. 6 - Expanded Load Ins. Loss Scan

The results of the expanded insertion loss scan on the 0.2 Ohm Load described in Figure Two as illustrated by Figure Six indicate that above approximately 1.050GHz, to 1.5GHz a deviation of as much as approximately 9db (as a nominal) was encountered. The results of this scan indicate that the load approximates 0.55 to 0.6 Ohms at 1.5GHz.

Oscilloscope System Measurement Response

Various frequency scans were taken to determine the uniformity of the 7104 Oscilloscope System as previously described. In the lowest voltage ranges, the 'scope was found to exhibit more response loss at 1.0 GHz than in the voltage settings utilized during this ESD effort. Accordingly, the measurement evaluations were centered for only the higher voltage settings (i.e., greater than 100mV/Div.) of the vertical amplifier. The curve below describes the response of the 7104 Oscilloscope, with the scan performed beyond the range stipulated as criteria by the manufacturer.

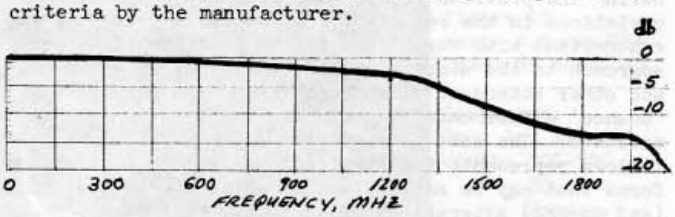

Fig. 7 - Frequency Response, 7104 System
Note: Loss at 2.6 GHz was 26db

A comparison of the frequency response curve yielded by the 1.0 GHz Oscilloscope System taken to 2.6 GHz to the insertion loss scan for the discharge 'load' provides the conclusion that the impedance increase of the load was partially compensating for the response loss from the Oscilloscope system. Accordingly, a net deviation profile became possible as an indicator of the response for the overall measurement system. It should be noted that the frequency response curve provided by Figure Seven, includes the insertion loss of the cable used for interconnection.

Combined Measurement System Response

The following curve approximates the net performance response deviation gathered by combining the effects of the insertion loss of the load and the response scan of the oscilloscope system with cable.

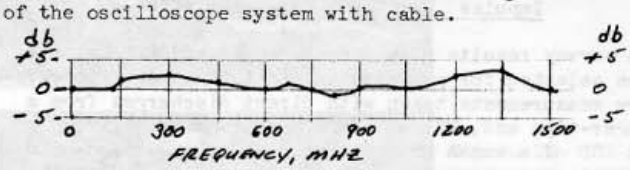

Fig. 8 - Net (Approximate) Response Deviation
Performance of Composite System

Based on the approximation provided by the graph of Fig. Eight, it can be recognized that the broadband response of the composite measurement system was generally within an envelope of -1db to +2db with the exception of the area centered on 300 MHz where the deviation was approximately +3db, and the area centered on approximately 1.3GHz where the deviation was approximately +3.9db. Although certainly not ideal, the authors believe that this overall response performance of the system is generally adequate to gather the desired ESD waveform characteristic data base within a reasonable accuracy given the unexpected dynamics of the data that is reported in this paper.

ESD Measurement Procedure

The foundation of the ESD waveform measurement method

(or approach) was relatively simple: Charge the human in evaluation to a known D.C. initialization level, and discharge the human through 'normal' contact to the ESD 'load' surface. During this process, the D.C. Voltmeter provided on the D.C. supply was monitored for the amount of deflection during the charging process to be certain that the human subject was brought up to the full desired level. Additionally, experiments were performed to ascertain that any significant amount of level was not dissipated between the point in time when the person left contact with the output of the power supply and the time of discharge to the load surface. Under the controlled relative humidity conditions of the facility, and with the person wearing the previously stated rubber-soled shoes, there was no significant dissipation encountered between the time points noted.

Discharge Motion, Velocity and Approach

During the previous (1979) study efforts, significant variations in the resultant ESD waveforms were observed concomitant with variations in the velocity of the approach to the discharge load, the angle of approach, and other attendant circumstances such as a mechanical 'bounce' effect once contact with the load plane was executed. The data presentation of this effort that follows represents the 'typical' variations in the waveforms that may be anticipated to exist due to the usual (and normal) alterations of velocity, motion and approach technique. As various waveforms were observed, multiple impulses were applied in sufficient quantities as derived from the human subject in order to capture waveforms on film that were indicative of all significant variations encountered at each incremental level.

ESD Waveform Measurement Environment

All measurements reported herein were taken under the relative humidity condition of 40% at a temperature of 70°F. During the evaluations, these values were held within a tolerance of 5% for relative humidity and temperature. It should be noted that preliminary tests have indicated that no significant waveform variation has been observed when the relative humidity level was altered between 20% and 60%, although these results are currently inconclusive due to the limited number of ESD impulse samples gathered.

Personnel Electrostatic Discharge: Impulse Waveform Characteristics

The survey results of two measurement conditions have been selected for presentation in this paper: ESD waveform measurements taken with direct discharges from a finger-tip; and, ESD waveform measurements derived from the ESD of a human that was holding a small hand-held metallic object that was intervening in the ESD path. Examples of such objects are keys, finger-rings, watchbands, coins, and small hand-held tools. This study was extended to include waveform characterizations of ESD through and from furnishings, such as push-carts and desk chairs, however limitations of available publication space do not permit inclusion of these measurements in this report.

Incremented Initialization Amplitude Approach

Empirical background gained from the previous studies had suggested that the dynamic waveform characteristics of personnel ESD were dramatically impacted by alterations of the initialization (charge) amplitude. These waveform alterations had been observed to be far more significant than simply increasing or decreasing the resultant amplitude of the actual impulse current peak and holding the fundamental risetime and pulse width as constants. These empirical observations had yielded the suggestion that in conjunction with significant changes in the fundamental waveshapes, a non-proportionality in the relationship between the initialization level and the peak impulse current ESD level was additionally possible. Accordingly, it was decided to perform this study as an exploration of the dynamic ESD waveforms by starting the measurements at relatively low initialization amplitudes (250 Volts to 500 Volts) and examining the alterations in impulse current and waveshape as the initialization amplitude was incrementally increased in steps found appropriate during the sequence of the measurement series.

Multiple Impulses and Periodicity of Sequence

As in the other effects, empirical efforts by the authors in antecedence to this study had illustrated the effect that multiple ESD impulses were possible, if not inherent, in what was usually perceived as a 'single' ESD impulse event. Within the confines of limited publication space, the periodicity and sequence of this aspect of the ESD phenomena is overviewed in this study. The following description of the multiple-impulse-event is suggested by the measurment results.

At initialization levels primarily above the 3kV to 4kV range, multiple ESD impulses appear to be caused by the following sequence, which has been found frequently under the condition of a discharge through a small metal object intervening in the ESD path. First, an initial ionization-based pulse is executed in the sequence. During the conduction through ionization time frame, the charge level on the human is rapidly decreasing. On occasion, the charge level is decreased through the discharge faster than the human velocity in motion can close the discharge gap to a point where the ionization path could be maintained. At some point in time and charge level, largely dependent on the velocity of gap closure, the ionization is extinguished due to the effect that the rate of gap closure does not track the decrease in amplitude. This results in a temporary interruption in the overall discharge process, until the gap becomes sufficiently small to enable a process of re-establishment of the ionization path, at a lower level, or until direct mechanical contact with the ESD load point is achieved. Once contact is made, added pulses are possible through a 'switch bounce' effect. Essentially the same phenomenon is possible in ESD of humans without metallic objects, but the quantity of multiple impulses and the probability of the effect is less in that there is less 'field enhancement' due to the shape of the finger-tip, and the compliant nature of human tissue minimizes the possibility of contact 'switch bounce'.

From the suggested sequence of multiple ESD impulses provided above, it may be recognized that since each individual impulse occurs at an incrementally reduced initialization-equivalent level, then the waveshape of each impulse should be correlatable to a primary waveform derived from a primary initialization level at the equivalent (as the reduction) amplitude. The results of this study confirm this contention in that all waveshapes of the sequence hold correlation to the primary waveshape of a reduced amplitude. It should also be recognized from this description that the ESD event may be executed as an event 'continuum'.

Incremental Level Measurements Human-Direct ESD

The following ESD waveform data base was gathered in discharges from a human finger-tip. Every attempt was made to present the envelope range of waveforms encountered, through the observation of thousands of ESD events, the photography of hundreds, and selection of the few presented in this paper. The person under evaluation executed the ESD through normal contact methods.

Human-Direct ESD: 500 Volts Initialization Level

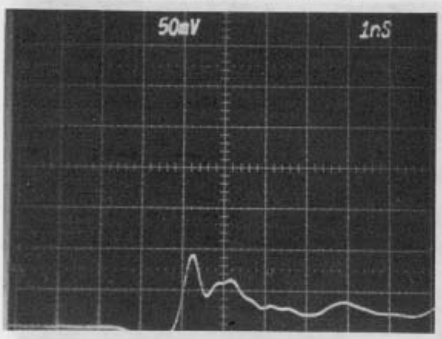

Figure 9
Vert: 0.5 Amp/Div.
Time: 1nSec/Div.

Displayed:
Ipeak: 0.9 Amps
Trise: 400pSec

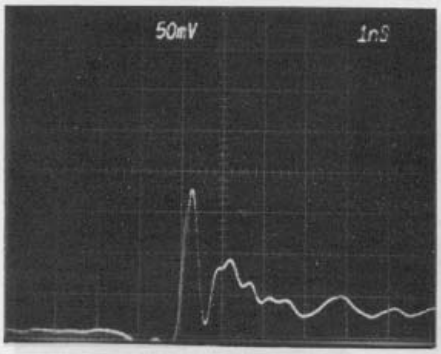

Figure 10
Vert: 0.5 Amp/Div.
Time: 1nSec/Div.

Displayed:
Ip : 1.8 Amps
Tr : 300 pSec.

Human-Direct ESD: 1,000 Volts Initialization Level

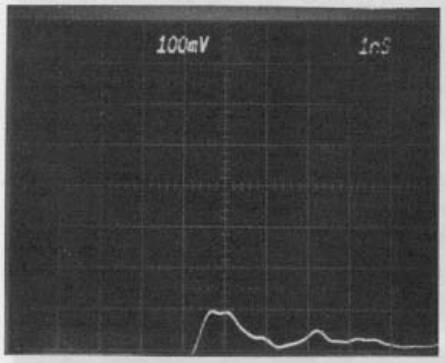

Figure 11
Vert: 1.0 Amp/Div.
Time: 1 nSec/Div.

Displayed:
Ip : 1.0 Amps
Tr : 500 pSec

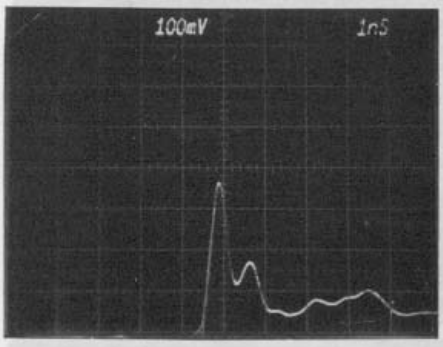

Figure 12
Vert: 1.0 Amp/Div.
Time: 1 nSec/Div.

Displayed:
Ip : 3.6 Amps
Tr : 250 pSec

Human-Direct ESD: 2,000 Volts Initialization Level

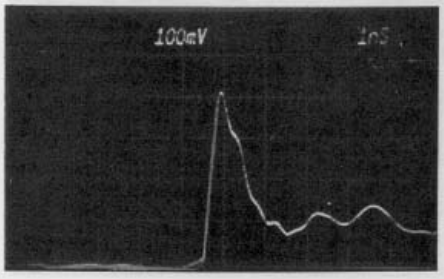

Figure 13
Vert: 1.0 Amp/Div.
Time: 1 nSec/Div.

Displayed:
Ip : 4.1 Amps
Tr : 200 pSec

(2kV, Cont.)

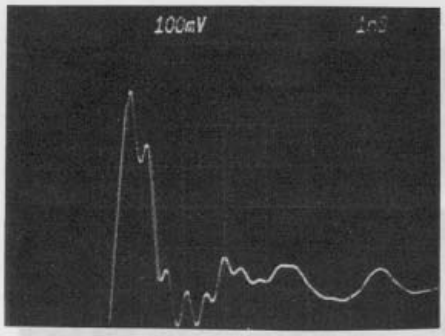

Figure 14
Vert: 1.0 Amp/Div
Time: 1 nSec/Div

Displayed:
Ip : 5.8 Amps
Tr : 300 pSec

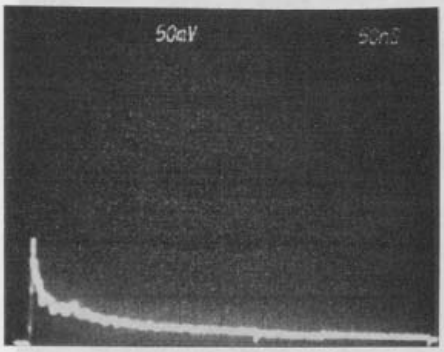

Figure 15
Vert: 0.5 Amp/Div
Time: 50 nSec/Div

Displayed:
Ip : 1.3 Amps
Width: 50%-50%
30 nSec
Approx.

Human-Direct ESD: 4,000 Volts Initialization Level

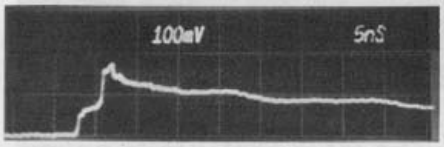

Figure 16
Vert: 1.0 Amp/Div
Time: 5 nSec/Div
Displayed:
Ip: 1.8 Amps

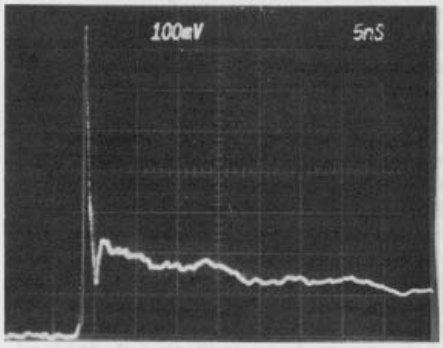

Figure 17
Vert: 1.0 Amps/Div
Time: 5 nSec/Div

Displayed:
Ip : 7.6 Amps
Tr : 400 pSec

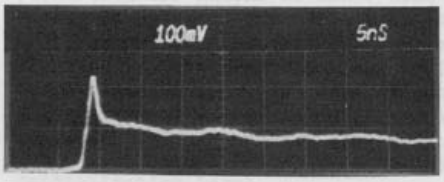

Figure 18
Vert: 1.0 Amp/Div
Time: 5 nSec/Div
Displayed:
Ip : 2.3 Amps
Tr : 2 nSec

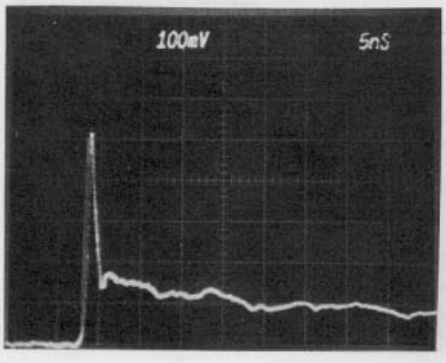

Figure 19
Vert: 1.0 Amp/Div
Time: 5 nSec/Div

Displayed:
Ip : 5.2 Amps
Tr : 1 nSec
Approx.

Human-Direct ESD: 6,000 Volts Initialization Level

Typical Waveforms:

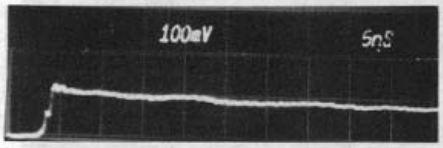

Figure 20
Vert: 1.0 Amps/Div
Time: 5 nSec/Div
Displayed:
Ip : 1.2 Amps
Tr : 1.5 nSec

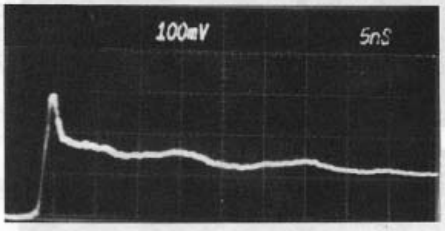

Figure 21
Vert: 1.0 Amps/Div
Time: 5 nSec/Div

Displayed:
Ip : 3.0 Amps
Tr : 1.5 nSec

Atypical Waveforms:

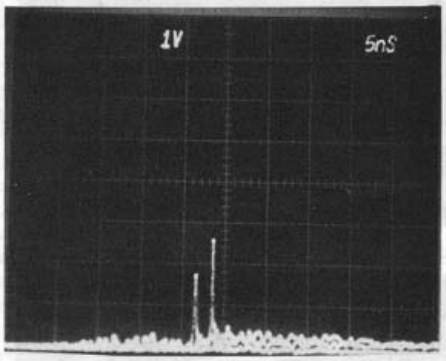

Figure 22
Vert: 10.0 A/Div
Time: 5 nSec/Div

Displayed:
Ip : 26 Amps

(Two pulse overlay)

Comment: The ultra-fast risetime, high current pulse at 6kV was attributable to fast human velocity in executing the ESD event. Although found too infrequently to photograph, the highest peak current encountered during human-direct ESD evaluations was observed with the waveform of Figure 22 above, at a peak amplitude of 60 Amps.

Transistion: The 6kV to 8kV initialization level area appeared to be a transistion point from ultra-fast risetime and high current events, to more predictable (or conventional) risetimes and peak currents. The data profiles across the incremental level results tends to suggest that: a) At low levels, the surface-to-surface localized distributions between hand & finger to load plane dominate the impulse execution; and, b) at higher initialization levels, the presence of increased ionization in the impulse path tends to extend the risetimes, which in turn permits more efficient transfer of conventional ESD levels from the storage capacitance between the feet and floor surface. This projection basis seems to gain credibility when the impulse base-widths are examined for events at and above 8kV initialization. These general projections are expanded in the description of a model circuit, later in this paper.

Human-Direct ESD: 8,000 Volts Initialization

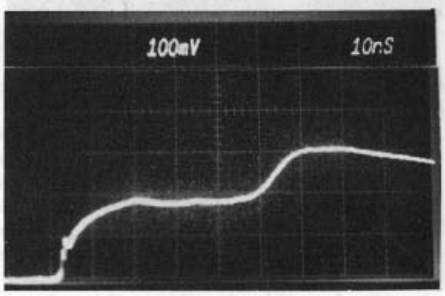

Figure 23
Vert: 1.0 Amps/Div
Time: 10. nSec/Div

Displayed:
Ip : 3.0 Amps
Tr : Complex, 55nS to peak

(8kV Continued)

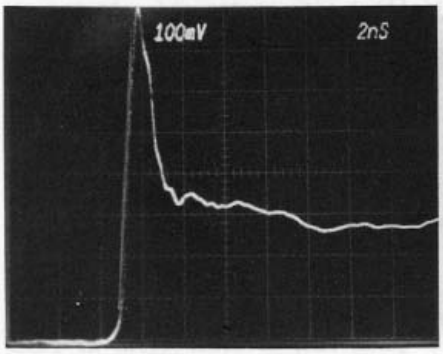

Figure 24
Vert: 1.0 Amp/Div
Time: 2 nSec/Div

Displayed:
Ip : 8 Amps
Tr : 1 nSec Approx.

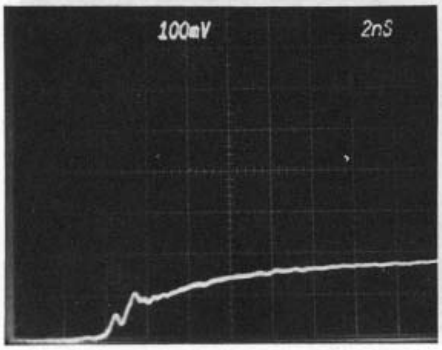

Figure 25
Vert: 1.0 Amp/Div
Time: 2 nSec/Div

Displayed:
Ip : 1.8 Amps
Tr : 6 nSec Approx.

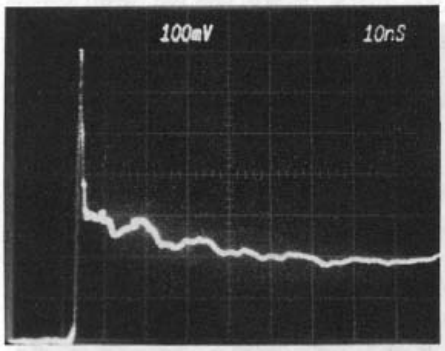

Figure 26
Vert: 1.0 Amp/Div
Time: 10 nSec/Div

Displayed:
Ip : 7 Amps
Tr: 2 nSec Approx.

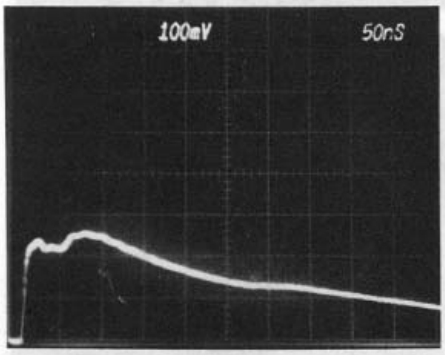

Figure 27
Vert: 1.0 Amp/Div
Time: 50 nSec/Div

Displayed:
Ip : 2.6 Amps
Width: 50%-50% 200 nSec Approx.

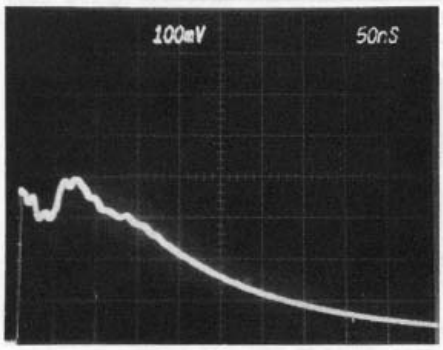

Figure 28
Vert: 1.0 Amp/Div
Time: 50 nSec/Div

Displayed:
Ip : 4 Amps
Width: 50%-50% 200 nSec Approx.

Human-Direct ESD: 10,000 Volts Initialization Level

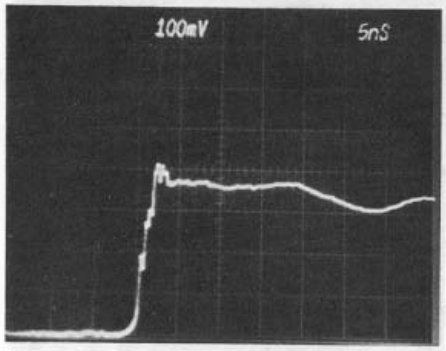

Figure 29
Vert: 1.0 Amp/Div
Time: 5 nSec/Div

Displayed:
Ip : 4.2 Amps
Tr : 2 nSec

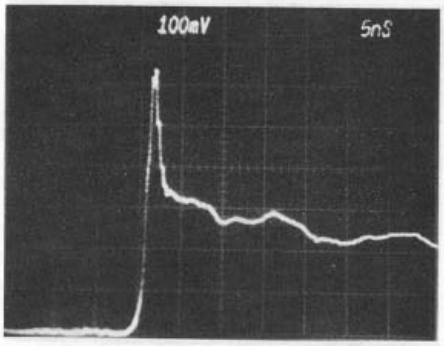

Figure 30
Vert: 1.0 Amp/Div
Time: 5 nSec/Div

Displayed:
Ip : 6.4 Amps
Tr : 2 nSec

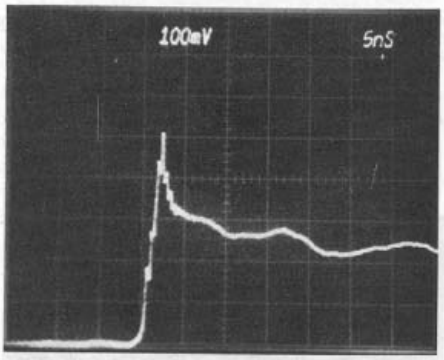

Figure 31
Vert: 1.0 Amp/Div
Time: 5 nSec/Div

Displayed:
Ip : 5.1 Amps
Tr : 2.5 nSec

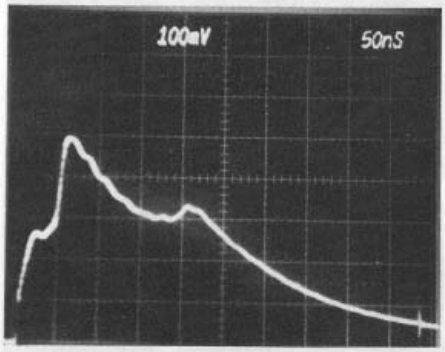

Figure 32
Vert: 1.0 Amp/Div
Time: 50 nSec/Div

Displayed:
Ip : 5 Amps
Tr : Complex, 60 nSec to peak
Width: 50%-50% 250 nSec

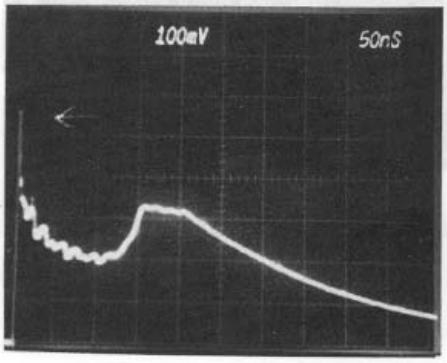

Figure 33
Vert: 1.0 Amp/Div
Time: 50 nSec/Div

Displayed:
Ip : 5.5 Amps (Contrast poor)
Tr : Fast
Width: 50%-50% 250 nSec

Human-Direct ESD: 15,000 Volts Initialization Level

Due to the discomfort level to the test personnel, only a comparatively small number of impulses were observed and sampled photographically at the 15kV level. Since the photographic recording process requires many pulse samples to actually record (on film) the envelope level range produced, it was decided to photograph only a typical waveform that was generally indicative of those observed, and to report other peak currents as a note of others seen.

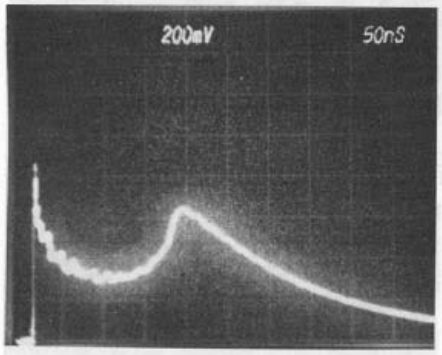

Figure 34
Vert: 2.0 Amp/Div
Time: 50 nSec/Div

Displayed:
Ip : 8.7 Amps
Width: 50%-50% 300 nSec Approx.

Peak Current Range: The observed peak current range for the 15kV initialization level was 5 to 15 Amps with essentially the waveshape of Figure 34 shown above.

Incremental Level Measurements Human ESD Through Small Metallic Objects Intervening In The ESD Path

Previous study efforts by the authors had indicated that the peak currents produced by the condition of an ESD of personnel through small hand-held metallic objects that intervened in the ESD path were very significantly more severe than the impulse currents produced by the human-direct ESD condition. In addition, the majority of digital-product manufacturers contacted by the authors during the past three years have indicated that since their products were constantly utilized by personnel that frequently contacted their products through small metallic objects (pens, coins, rings), the manufacturers preferred to evaluate the products only in tests to the worst-case condition: ESD of humans through small metallic objects. These manufacturers have been adjusting their corporate standards to test for product performance under simulation of this condition. The data that follows indicates the validity of the conclusion that the ESD of a human with a metal object is significantly the worst-case condition when compared to the waveforms of ESD from human direct contact provided above.

Human ESD Through Small Metallic Objects: 250 Volts Initialization Level

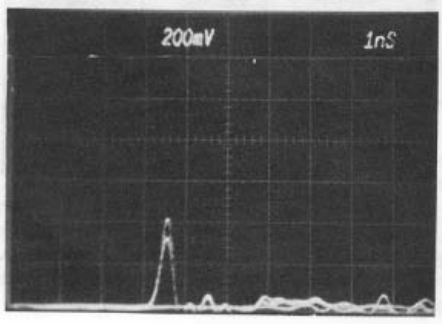

Figure 35
Vert: 2 Amp/Div
Time: 1 nSec/Div

Displayed:
Ip : 4 Amps
Tr : 250 pSec Approx.
Width: 500 pSec Approx.
(2 pulse overlay)

Human ESD Through Small Metallic Objects: 500 Volts Initialization Level

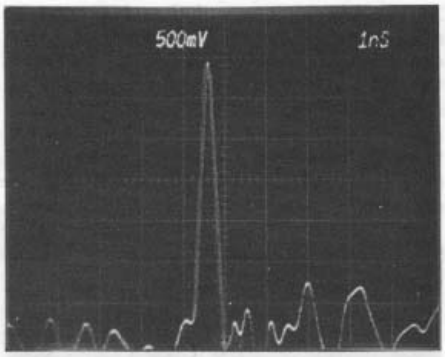

Figure 36
Vert: 5 Amps/Div
Time: 1 nSec/Div

Displayed:
Ip : 34 Amps
Tr: 250 pSec
Approx.
Width: 400 pSec
Approx.

Human ESD Through Small Metallic Objects: 1,000 Volts Initialization Level

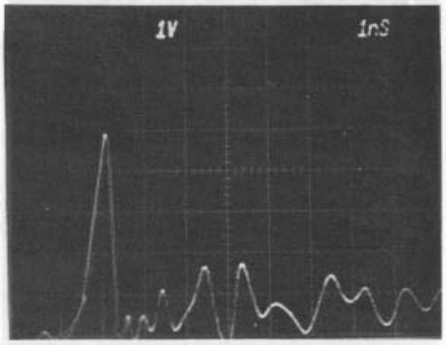

Figure 37
Vert: 10 Amps/Div
Time: 1 nSec/Div

Displayed:
Ip : 50 Amps
Tr: 500 pSec
Width: 500 pSec
Approx.

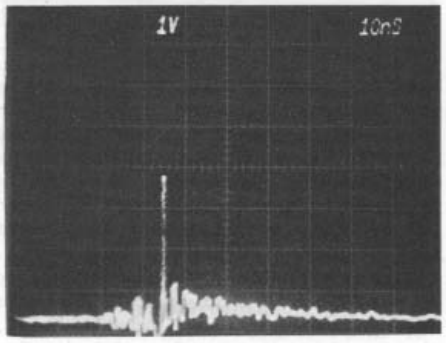

Figure 38
Vert: 10 Amps/Div
Time: 10 nSec/Div

Displayed:
Ip : 36 Amps

It should be noted that Figure 38 is provided to show the ratio of the ultra-fast "spike" amplitude to the otherwise low-level basewidth current.

Human ESD Through Small Metallic Object: 2,000 Volts Initialization Level

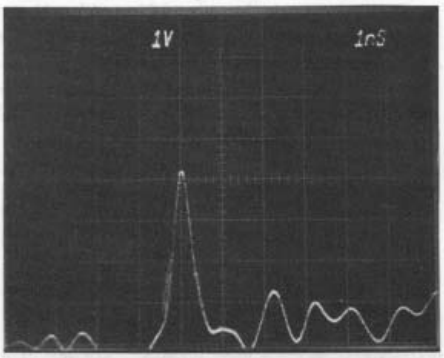

Figure 39
Vert: 10 Amps/Div
Time: 1 nSec/Div

Displayed:
Ip : 42 Amps
Tr : 500 pSec
Width: 50%-50%
450 pSec

A comparison of this 2kV-derived level to the data shown in Figure 40 yields indications of the typical variation in peak current that is experienced from event-to-event. As shown in Figure 41, the ratio of "spike" to basewidth current is still very high at the 2kV level.

(2,000 Volts Continued)

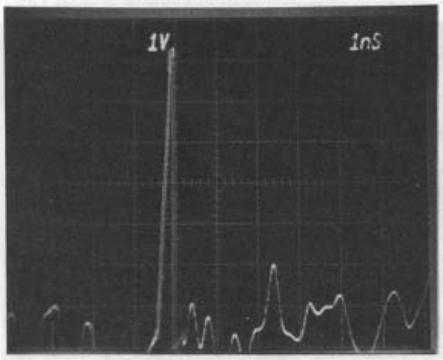

Figure 40
Vert: 10 Amps/Div
Time: 1 nSec/Div

Displayed:
Ip : 74 Amps
Tr : 200 pSec
Width: 50%-50%
250 pSec
Approx.

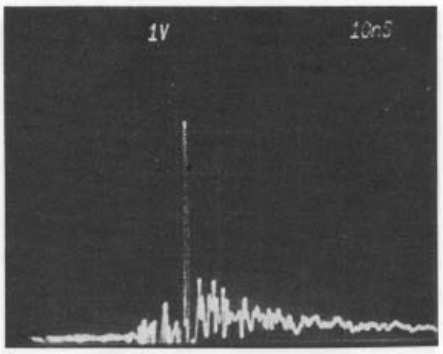

Figure 41
Vert: 10 Amps/Div
Time: 10 nSec/Div

Displayed:
Ip : 53 Amps
Note small base width current.

Human ESD Through Small Metallic Object: 4,000 Volts Initialization Level

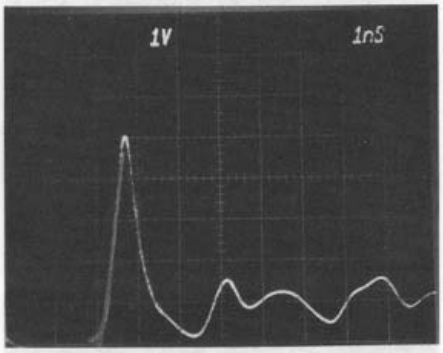

Figure 42
Vert: 10 Amps/Div
Time: 1 nSec/Div

Displayed:
Ip : 50 Amps
Tr : 500 pSec
Width: 50%-50%
500 pSec
Approx.

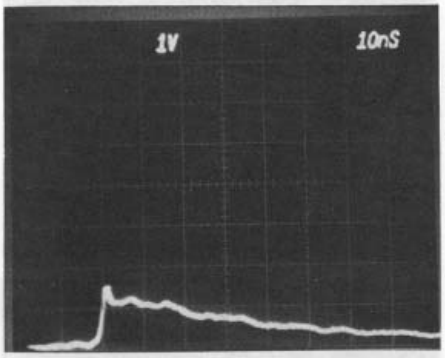

Figure 43
Vert: 10 Amps/Div
Time: 10 nSec/Div

Displayed:
Ip : 15 Amps
Tr : 1 nSec
Approx.
Width: 50%-50%
50 nSec

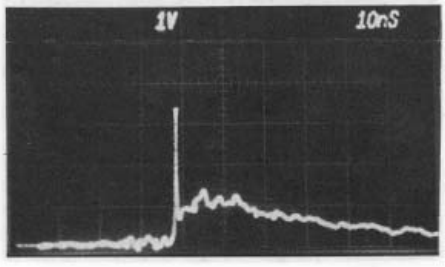

Figure 44
Vert: 10 Amps/Div
Time: 10 nSec/Div

Displayed:
Ip : 35 Amps
Otherwise Complex

(4,000 Volts Initialization - Continued)

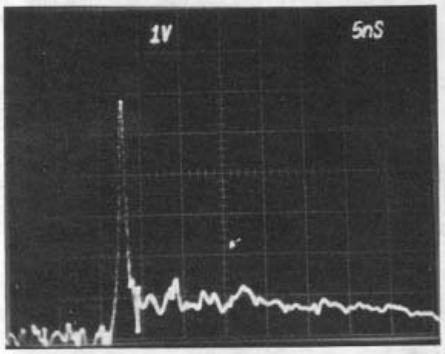

Figure 45
Vert: 10 Amps/Div
Time: 5 nSec/Div

Displayed:
Ip : 58 Amps
Tr: 1.5 nSec
Approx.
Width: Complex

From the data base of Figures 42 through 45 above, it may be recongized that the 4,000 Volt initialization level resulted in a complex series of slower-risetime ionization-caused impulses, and the fast-risetime events that we have characterized as being associated with the localized surface-to-surface distribution effects. In fact, the 4,000 Volt initialization level exhibited many of the "transitional" characteristics that were described for the 6,000 Volt initialization level in the human direct ESD event series (subsequent to Figure 22). At that level in the human-direct series, rather enormous peak currents were infrequently observed (Figure 22). The phenomenon of enormous peak currents was also observed at the 4kV level for the Human-with-metallic-object condition, which is now projected as the transistional level of this condition by the authors. The non-proportionality, if not enormity, of the possible ESD impulse current at the 4,000 Volt initialization level is manifested in this data base by the following Figures, albeit an infrequent event. To bring the impulse levels into measurement range, a wideband 20db attenuator was added to the measurement arrangement.

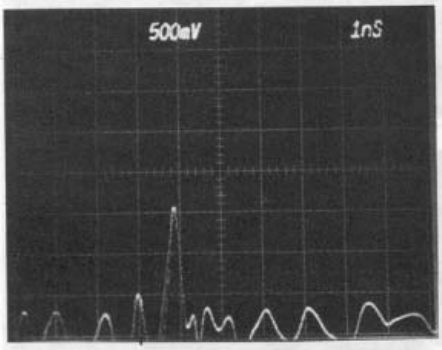

Figure 46
Vert: 50 Amps/Div
Time: 1 nSec/Div

Displayed:
Ip : 160 Amps
Tr : 300 p Sec
Width: 50%-50%
300 pSec

Note: 20db Atten in circuit.

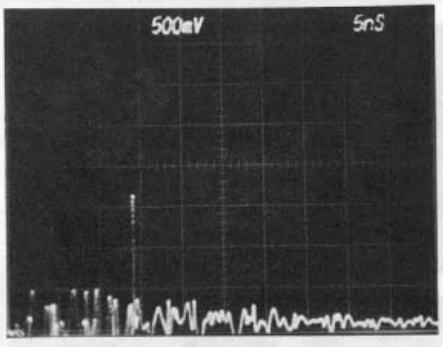

Figure 47
Vert: 50 Amps/Div
Time: 5 nSec/Div

Displayed:
Ip : 170 Amps
Note: High ratio to base current

It should be noted that 170 Amperes of peak current was actually the highest observed for this series at the 4 kV initialization level, indicating that this photograph shows the worst-case level encountered.

Assuming that the 4kV initialization level is actually the projected 'transistional' level for this impulse condition, then extended risetimes should be realized above this level commensurate with the increased development of ionization in the ESD path.

Human ESD Through Small Metallic Object: 6,000 Volts Initialization Level

Note: 20db Attenuator retained in the 'scope input.

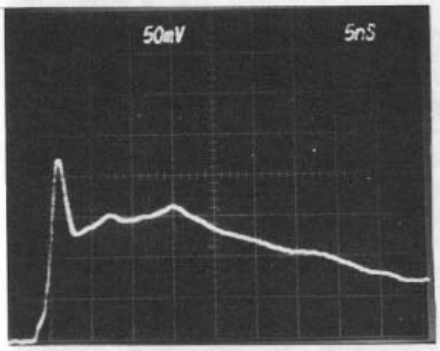

Figure 48
Vert: 5 Amps/Div
Time: 5 nSec/Div

Displayed:
Ip : 22 Amps
Tr : 2 nSec

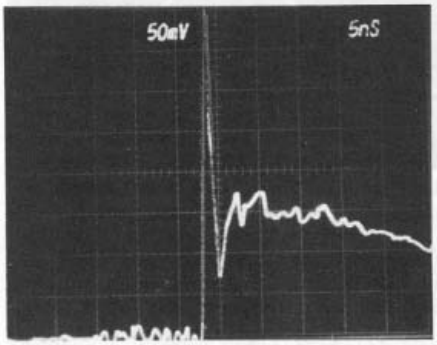

Figure 49
Vert: 5 Amps/Div
Time: 5 nSec/Div

Displayed:
Ip : 40+ Amps
Tr : 500 pSec
Approx.

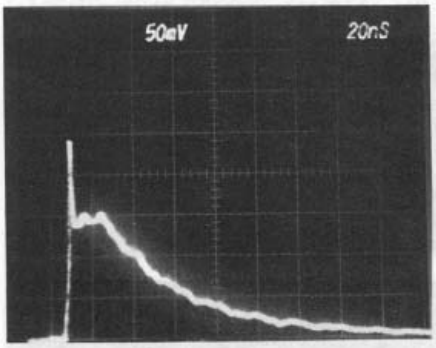

Figure 50
Vert: 5 Amps/Div
Time: 20 nSec/Div

Displayed:
Ip : 24 Amps
Width: Complex,
50%-50%
40 n Sec

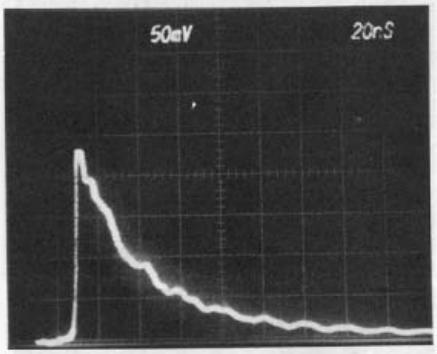

Figure 51
Vert: 5 Amps/Div
Time: 20 nSec/Div

Displayed:
Ip : 23 Amps
Width: 50%-50%
30 nSec
Approx.

From these data provided above, it can be recognized that increased effects, presumably from ionization, are generally extending the risetimes.

Additionally, it may be concluded that the 6kV level in this 'metallic object' condition is approximately analogous to the 8kV level under the human-direct condition.

Human ESD Through Small Metallic Object: 7,500 Volts Initialization Level

An exarple of multiple impulse structures, as derived from a single initialization level, was recorded at 7,500 Volts for informational purposes. It should be noted that many photographic demonstrations were possible after the initialization level of 4kV was achieved. This example taken at 7.5kV is arbitrarily selected for display.

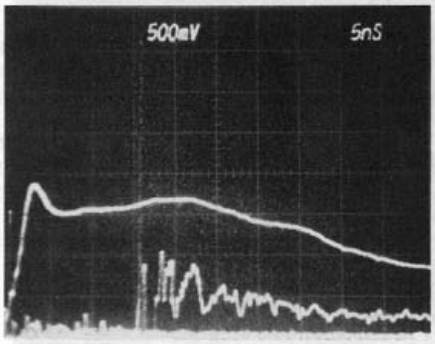

Figure 52
Vert: 5 Amps/Div
Time: 5 nSec/Div

Display: Multiple Impulses from one Charge level.

Figure 52 above illustrates three separate ESD events that were derived from a single initialization level (charge). The first event is ionization-based, exhibiting a risetime of approximately three nanoseconds and a peak current of 19 Amperes. The second event is significantly displaced in time, and appears about three divisions from the left side. This is a very narrow width pulse, exhibiting a 37 Ampere peak current. The third event is also displaced in time, appearing about ¼ of the first division from the time zero position. This tertiary impulse exhibits a 16 Ampere peak current level, and is probably due to a 'bounce' effect.

Human ESD Through Small Metallic Object: 8,000 Volts Initialization Level

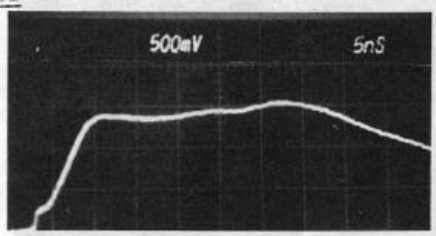

Figure 53
Vert: 5 Amps/Div
Time: 5 nSec/Div

Displayed:
Ip : 15 Amps
Tr : 5 nSec

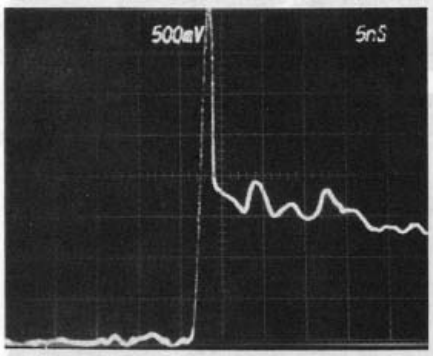

Figure 54
Vert: 5 Amps/Div
Time: 5 nSec/Div

Displayed:
Ip : 40 Amps
Tr : 1 nSec

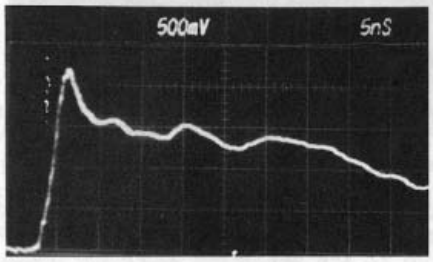

Figure 55
Vert: 5 Amps/Div
Time: 5 nSec/Div

Displayed:
Ip : 22 Amps
Tr : 2 nSec

(8,000 Volts Initialization Continued)

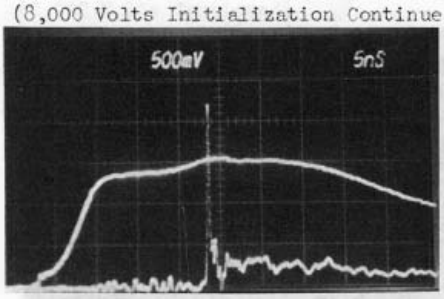

Figure 56
Vert: 5 Amps/Div
Time: 5 nSec/Div

Displayed:
Ip : 15 Amps
Ip #2 : 22 Amps
Tr : 5 nSec
Tr #2: Ultra-Fast

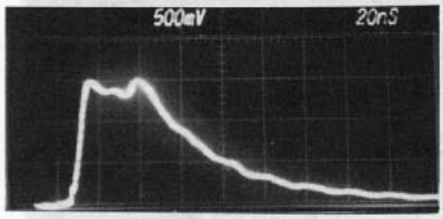

Figure 57
Vert: 5 Amps/Div
Time: 20nSec/Div

Displayed:
Ip : 15 Amps
Tr : 5 nSec
Width: 60 nSec
(50%-50%)

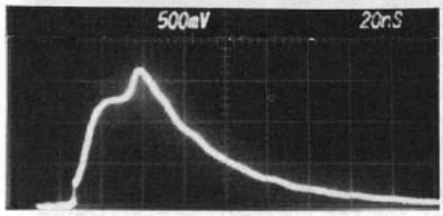

Figure 58
Vert: 5 Amps/Div
Time: 20 nSec/Div
Displayed:
Ip : 17 Amps
Tr : 30 nSec
Width: 60 nSec
(50%-50%)

Human ESD Through Small Metallic Object: 10,000 Volts Initialization Level

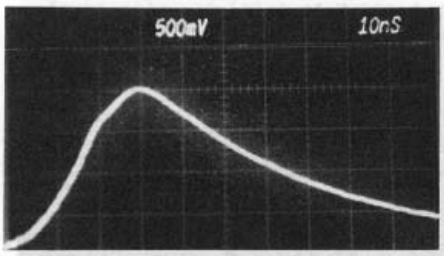

Figure 59
Vert: 5 Amps/Div
Time: 10 nSec/Div
Displayed:
Ip : 20 Amps
Tr : 20 nSec
Width: 50%-50%
50 nSec

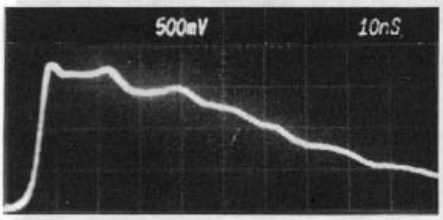

Figure 60
Vert: 5 Amps/Div
Time: 10 nSec/Div
Displayed:
Ip : 17 Amps
Tr : 4 nSec
Width: 50%-50%
70 nSec

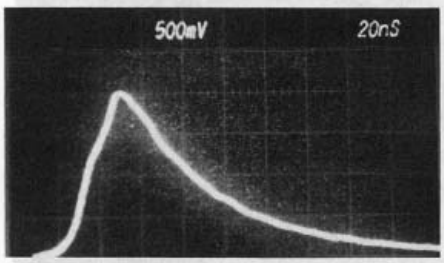

Figure 61
Vert: 5 Amps/Div
Time: 20 nSec/Div
Displayed:
Ip: 20 Amps
Tr: 20 nSec
Width: 50%-50%
60 nSec

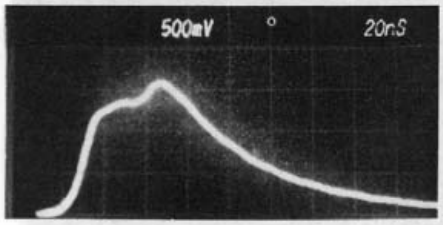

Figure 62
Vert: 5 Amps/Div
Time: 20 nSec/Div
Displayed:
Ip : 16 Amps
Tr : 40 nSec,
Complex
Width: 50%-50%
80 nSec

The data base provided above in Figures 59 through 62 indicates that once substantial ionization becomes present in the ESD path, the stability of the amplitude improves somewhat, other than for the potential effects of multiple impulses as previously described. The variations in the risetime are believed to be caused by small alterations in the path of the ionization from pulse-to-pulse.

Human ESD Through Small Metallic Object: 12,500 Volts Initialization Level

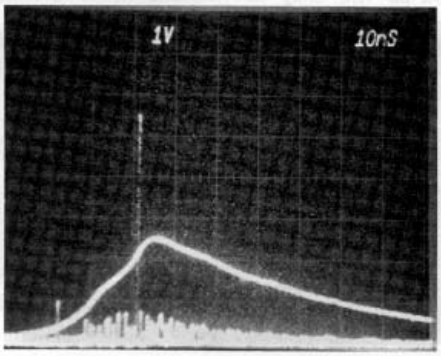

Figure 63
Vert: 10 Amps/Div
Time: 10 nSec/Div
Displayed:
Ip #1: 25 Amps
Ip #2: 55 Amps
Ip #3: 10 Amps
Tr #1: 20 nSec

Width #1: 50%-50%
50 nSec

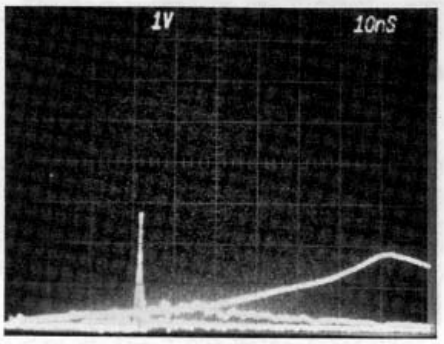

Figure 64
Vert: 10 Amps/Div
Time: 10 nSec/Div
Displayed:
Ip #1: 18 Amps
Ip #2: 28 Amps
Tr #1: 60 nSec

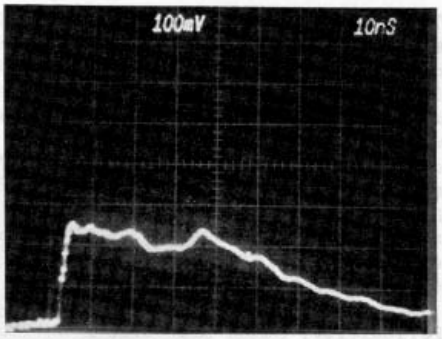

Figure 65
Vert: 10 Amps/Div
Time: 10 nSec/Div

Displayed:
Ip : 25 Amps
Tr : 2 nSec
Approx.

Note: 20db Atten
at 'scope
for this
photograph

The 12.5kV initialization level data gathered above for Figures 63 and 64 (only) were taken using the fastest "rapid" human velocity during the approach to the load. In this example, the rapid velocity tended to increase the probability of multiple impulses.

Human ESD Through Small Metallic Object: 15,000 Volts Initialization Level

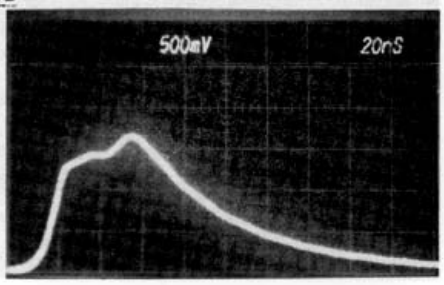

Figure 66
Vert: 5 Amps/Div
Time: 20 nSec/Div
Displayed:
Ip : 17 Amps
Tr : 10 nSec
Approx.
Width: 70 nSec
50%-50%

(15,000 Volts Initialization Continued)

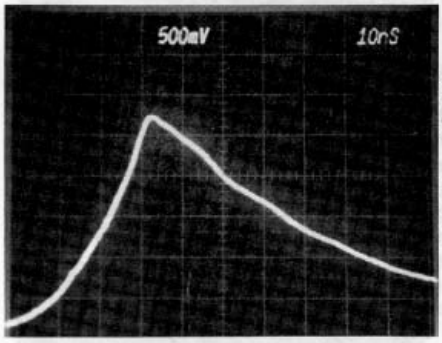

Figure 67
Vert: 5 Amps/Div
Time: 10 nSec/Div

Displayed:
Ip : 28 Amps
Tr : 25 nSec
Width: 55 nSec
50%-50%
Approx.

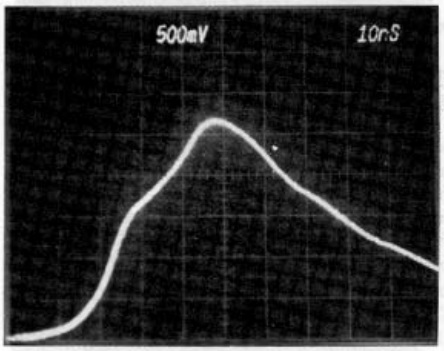

Figure 68
Vert: 5 Amps/Div
Time: 10 nSec/Div

Displayed:
Ip : 27 Amps
Tr : 30 nSec
Width: 60 nSec
50%-50%
Approx.

As may be recognized from previous patterns, the ESD impulse current tends to stabilize somewhat when significant amounts of ionization are present in the ESD path. The 15kV data above, illustrates this effect.

Human ESD Through Small Metallic Object: 20,000 Volts Initialization Level

Due to the discomfort level of test personnel at the 20 kV initialization level, only a few impulse samples were monitored. It is significant to note, however, that of the several impulse sample observed, all pulses repeated within approximately ±10% of the representation of Figure 69 below. It is suggested that this stabilizing effect is due to the human motion at the 'discomfortable' level operating in conjunction with the stabilizing effect of the extended ionization path length.

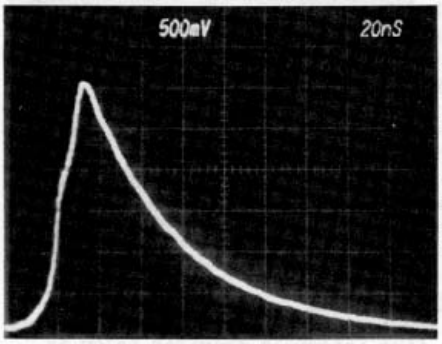

Figure 69
Vert: 5 Amps/Div
Time: 20 nSec/Div

Displayed:
Ip : 31 Amps
Tr : 20 nSec
Width: 50%-50%
45 nSec

Nonproportionality of impulse peak currents may be recognized for the longer-risetime ionization-based ESD events, by making a comparison between the waveforms of the 10kV Figure 61 against the 20kV pulse example of Figure 69. At 10kV, an approximately similar waveshape produced a peak current of 20 Amperes, while the 20kV example resulted in a peak current of only 31 Amperes, rather than the proportional level of 40 Amps. Increased path impedance due to arc length is usually

responsible for this characteristic of nonproportionality, in that the **arc** length at 20 kV is obviously longer than the arc length at 10kV, adding series impedance.

Photographic Data Compression

It should be noted that some of the photographic data examples provided herein were cropped for unnecessary graticule size in order to 'compress' the total height occupied in the columns. This editorial measure was taken in order to conserve the available publication space. When executed, the original graticule legends were replaced on the top of each photograph. The waveforms were never distorted to achieve this compression, only removal of unnecessary graticule size occuring between the top of the waveform display and the identification legends on the 'scope display was utilized as an editorial measure.

Multiple ESD Impulses: Event Periodicity & Sequence

The data base provided in the previous sections of this study report contains various examples of the existence of multiple ESD impulses that were derived from a single initialization level and 'discharge action'. On the fourth page of this paper, a discussion of the suggested sequence, cause and development of these multiple impulses has been included. With the acceptance of the existence of the multiple-**pulse phenomenon, however** probable, the question of the time spacing between each impulse within the overall event series emerges as a dominant consideration for further measurement study. The authors believe that information related to this spacing, or impulse periodicity, may be of particular interest to those concerned with ESD damage evaluations of sensitive devices such as semiconductors. Acting on that direction, the following experimental series was performed.

Periodicity: Measurement Technique

Preliminary measurements had indicated that the interval between the ESD events was substantially longer than the impulse width of any individual pulse within the event series. Various measurement experiments were performed as attempts to 'capture' the total impulse 'train' on a single CRT sweep, all without success due to the large ratio of impulse-width-to-interval. Accordingly, a measurement system was established, using the Tektronix 7104 Oscilloscope System, whereby each gate pulse of the time base trigger could be displayed. The 7104 was adjusted to display, and trigger from, the fastest and slowest events, in order that each trigger pulse from the time base could be photographed in a sequence for a multiple impulse series such as that depicted by Figures 52, 63, and 64. It should be noted that in performing these measurements, the full range of possible time base envelope frames were explored (from a few nanoseconds to a second) in order to be certain that all 'gates' of a sequence were recorded within the context of the sequence.

Periodicity: Data Presentation

The data of impulse time intervals provided below is actually the display of the trigger gate pulses from the 7104 Oscilloscope System. Accordingly, the only significant parameter to observe and consider is the time period between the impulses, not the amplitude and waveshape. During these tests, the 7104 was monitored to assure that the trigger pulses were actually caused by ESD **impulses** within each ESD event continuum.

Periodicity: Human-Direct ESD Events

As stated in the segment on the fourth page of this paper describing periodicity effects, the general observations gathered during these studies indicated that the probability of multiple impulses occuring during the human-direct ESD event condition was significantly less than for the human-with-small-metallic-object condition. This statement was true to the extent that the authors experienced difficulty in developing the multiple impulses in this 'human-direct' condition with sufficient regularity to permit photographic display. By reason of this difficulty factor, the following limited sample taken from a 2,000 Volt initialization level is presented as the only display for this condition.

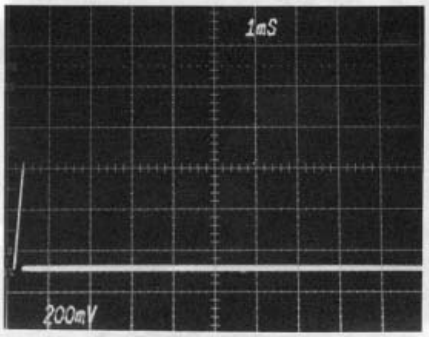

Figure 70

Time: 1 mSec/Div

Displayed:

One-Impulse Example - 10mSec Viewed.

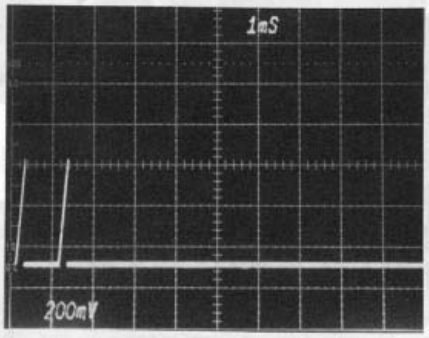

Figure 71

Time: 1 mSec/Div

Displayed: Two-Impulse Example - 10 mSec Viewed, 1.1mSec Interval

The data provided above illustrates an example of a single pulse at 2kV initialization, and an example of a double-pulse at 2kV. The time interval between each impulse within the double-pulse sequence was 1.1 milliseconds, which is an enormous time compared to the width of the largest pulse found for this level and condition which was between 100 and 200 nanoseconds as shown in Figure 15 for the width at the base. It is possible that the human-direct condition would produce a higher probability of multiple impulses at significantly higher initialization levels due to the increased path length dependency of ionization.

Periodicity: Human ESD Through Small Metallic Object

The following data photographs display various impulse sequences that were selected to overview the intervals and general periodicity of this ESD condition. The authors found that above approximately 4kV, the single pulse occurrence tended to be an exception rather than the normal event. The data is sampled through various initialization levels found appropriate for display.

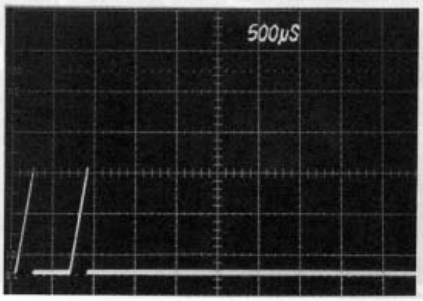

Figure 72
1,000 Volts Initialization

Time: 500uSec/Div

Displayed: Two pulse example, 650uSec interval, 5 mSec Viewed.

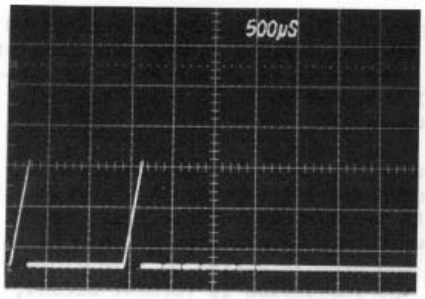

Figure 73
1,000 Volts
Initialization

Displayed: Two pulse example, 1.35 mSec interval 5 mSec viewed.

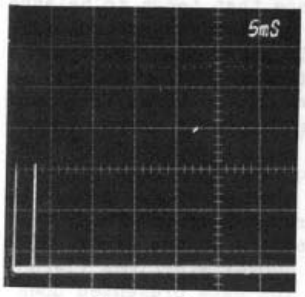

Figure 74

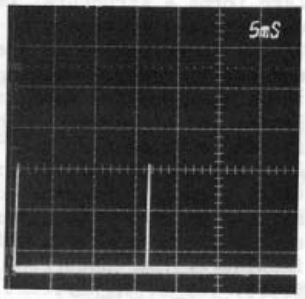

Figure 75

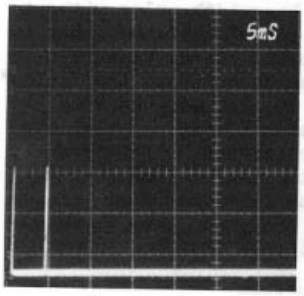

Figure 76

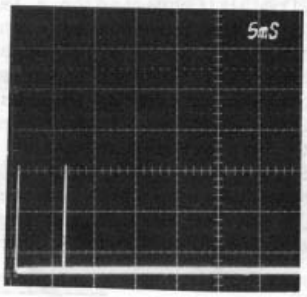

Figure 77

Examples of periodicity at the 2,000 Volts initialization level are provided by Figures 74 through 77 above. Although single pulses are possible, these examples show the full range measured, 2mSec to 15.7mSec. The photos have been cropped to remove unnecessary graticule. The full range of 50mSec was viewed originally.

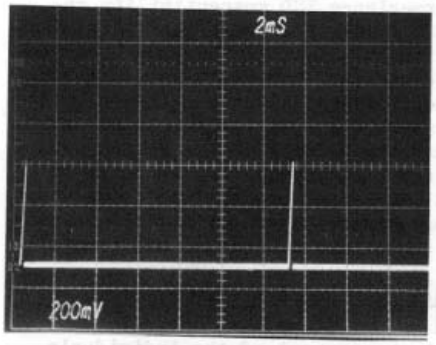

Figure 78
5,000 Volts
Initialization

Displayed: Two pulse example, 13mSec interval, 20mSec viewed.

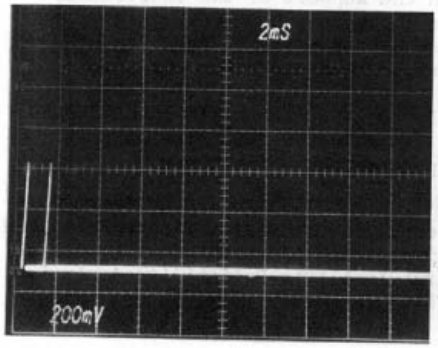

Figure 79
5,000 Volts
Initialization

Displayed: Two pulse example, 1.4mSec interval, 20mSec Viewed

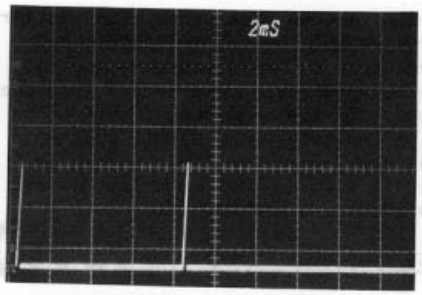

Figure 80
5,000 Volts
Initialization

Displayed: Two pulse example 8mSec interval 20mSec viewed

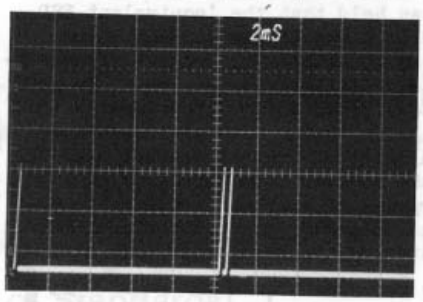

Figure 81
5,000 Volts
Initialization

Displayed: Three pulse example 10mSec-0.8mSec interval sequence, 20mSec viewed

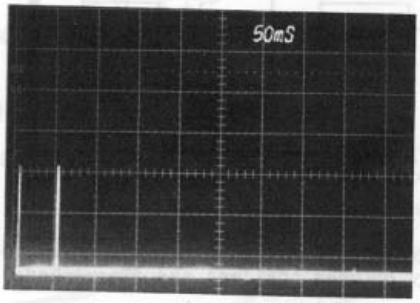

Figure 82
10,000 Volts
Initialization

Displayed: Two pulse example, 45mSec interval, 500mSec Viewed.

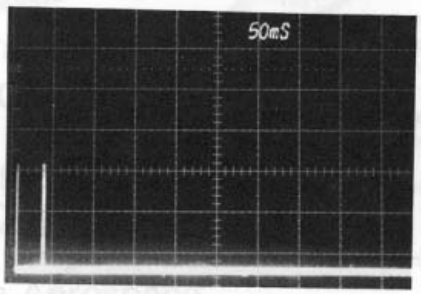

Figure 83
10,000 Volts
Initialization

Displayed: Two pulse example, 30mSec Interval, 500mSec Viewed.

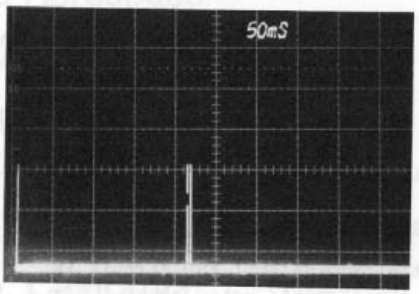

Figure 84
10,000 Volts
Initialization

Displayed: Three pulse example, 210mSec-10mSec interval sequence, 500 mSec viewed.

Periodicity: Indications

Generally, the periodicity measurements provided above indicate that the ratio of **the smallest time interval to the wider ESD pulse widths is in the order of** approximately 3,250:1, using the 650 microsecond spacing of Figure 72 to the 200 nanosecond width of Figure 15, a mixture of 1kV and 2kV results. Using the 10kV examples of a 10mSec spacing (Figure 84, 2nd event) and the 180 nanosecond basewidth of Figure 62, a ratio of approximately 55,000:1 is yielded. Obviously, the ratio becomes wider when the very narrow low voltage initialization pulses are considered as the probable

basis for the 2nd-impulse events that occur with smaller intervals. With very slow ESD contact velocities and high initialization voltages it was found that the 2nd pulse events could be delayed beyond one second from the initial 'time zero' pulse of the sequence. The conclusion gained from the periodicity data, albeit limited, is that the sequential displays of multiple pulses are sufficiently displaced in time so that each impulse of the series can be viewed as a single-acting event.

Conceptual ESD Composite Circuit Model

Conventional wisdom has held that the 'equivalent ESD circuit' is comprised of a capacitive element value connected to ground, as the storage component, discharged to a load through a resistive element value, in representation of the 'body resistance'. Considering the measurement condition of a 'human with small metallic object', which the majority of digital product manufacturers contacted by the authors have expressed an interest toward for purposes of systems products evaluation and criteria, the following composite circuit model is advanced as suggested by the results of this study.

Figure 85: Suggested Network

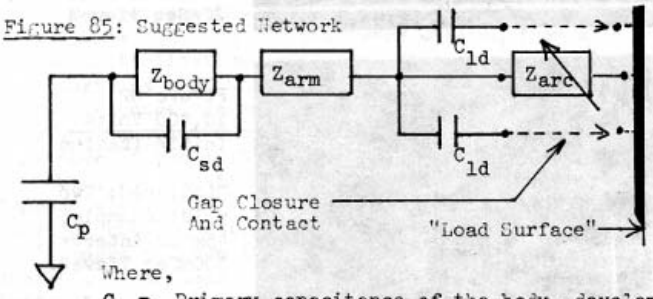

Where,

C_p = Primary capacitance of the body, developed broadly between the feet and floor planes

C_{sd} = Surface-to-surface parallel capacitance between the vertical surfaces and the parallel product planes

C_{ld} = Local surface-to-surface distributions of capacitance between the hand with object (or finger) and the immediate local surface under ESD exposure

Zbody = The structural impedance of the legs, torso, viewed as a series element

Zarm = Series impedance of the arm

Zarc = Series ionization path impedance of the arc, a variable with time and rate of re-initialization

Circuit Model: Proposed Equivalent Operation

It is suggested that the 'equivalent' ESD circuit is actually comprised of the segments noted above. For purposes of description, consider first that the human hand represents a distributive capacitance above a plane between approximately 1pfd and 20pfd, typically 5pfd, depending on the angle of incidence above the plane in the axis of the finger. This segment is 'Cld' and may be viewed as a sphere above a plane yielding a surface-to-surface distribution. Next, consider that the impedance of the arm, Zarm, is a relatively high number as compared to the impedance of the ionization path, Zarc, at low voltages when Zarc is inherently small. For low initialization levels, then, the largest current propagated will flow from the local storage element, Cld, through the low path impedance of Zarc. Under this condition, the small-value of current propagated through the impedance, Zarm, is generally neglectable when compared to the local impulse current derived through Cld, all of which results in the ultra-fast risetimes and very narrow pulses such as illustrated in Figures 10, 14, 17, 36-42, 45-47, with others also evident.

Continuing the ESD process into higher initialization levels requires an increased introduction of the path impedance Zarc. It is proposed that two effects occur that are associated with this Zarc introduction. First, it is suggested that the dynamic action of Zarc slows down the risetime as the ionization is formed. Second, Zarc forms a structural impedance that tends to balance out with the impedance of Zarm and Zbody, particularly in the lower ranges of spectral energy distribution across frequency. Assuming that Zarm (and/or Zbody) forms an impedance that is lower in the lower frequency range, and higher in the higher frequency range, then it can be recognized that with the introduction of the longer (and thereby, lower-frequency displaced) risetimes through the formation of the ionization path, the ability of energy transfers through Zarm and Zbody becomes more pronounced, which results in the wider ESD impulse widths concurrent with longer risetimes (1-2nS plus). It is significant that the data presented does not illustrate a sub-one-nanosecond risetime that is directly connected to a larger basewidth pulse without first the presence of a sharp 'spike' overshoot that is projected to be attributable to the energy transfer from Cld. In such examples that demonstrate the 'spike' overshoot, such as Figures 17, 19, 24, 26, 44, 49 & 54, it is suggested that a combination of factors minimized the extensive development of ionization, allowing the initial energy impulse to first transfer from Cld, and subsequent to that transfer, the remaining energy in Cp and Csd transferred through Zbody and Zarm to form the larger-width-but-lower-amplitude impulse.

Summary Conclusions

The ESD event series, networks, and network functions that are responsible for the production of the event series, appear to be substantially more complex and dynamic than had been previously considered by the authors. In particular, we believe the possibility exists that advanced digital systems and products that are (or will be) equipped with operative bandwidths which are capable of circuit responses in the hundreds of picoseconds may experience ESD susceptibility response to 'actual' ESD events that many test simulators are not capable of simulating, simply because their design base did not include the fast-event waveform complexity now recognized. Empirical data gathered by the authors in actual systems susceptibility response evaluations have confirmed the premise that a system will exhibit essentially equal susceptibility response to test simulators that can reproduce the waveforms delineated in this study, as compared against the susceptibility levels and conditions of 'actual ESD events'.

Acknowledgements

This has been an 'unfunded' study that has been made possible only through the support of the individuals noted here. For their cooperation, we wish to express our profound gratitude. They are: Mr. Paul Rey of Digital Equipment Corp., Maynard, Mass.; and, Mr. Demetrios Lignos, of Digital Equipment Corp. at Colorado Springs, Colorado. Our thanks to David Stanis of Cornell-Dubilier, Santa Monica Cal., for support with photographic reproductions. Thank you.

Reference (1): Ming, W. Michael, "Dynamic Waveform Characteristics of Personnel Electrostatic Discharge", 1979 Proceedings, Elect. Overstress-Electrostatic Discharge Symposium, ITT Research Institute-Reliability Analysis Center, EOS-1, Pgs 78-87, Rome Air Delv Center, Rome, New York.